A Generalized RAKE Receiver for Interference Suppression

Gregory E. Bottomley, *Senior Member, IEEE*, Tony Ottosson, *Member, IEEE*, and Yi-Pin Eric Wang, *Member, IEEE*

***Abstract*—Currently, a global third-generation cellular system based on code-division multiple-access (CDMA) is being developed with a wider bandwidth than existing second-generation systems. The wider bandwidth provides increased multipath resolution in a time-dispersive channel, leading to higher frequency-selectivity. In this paper, a generalized RAKE receiver for interference suppression and multipath mitigation is proposed. The receiver exploits the fact that time dispersion significantly distorts the interference spectrum from each base station in the downlink of a wideband CDMA system. Compared to the conventional RAKE receiver, this generalized RAKE receiver may have more fingers and different combining weights. The weights are derived from a maximum likelihood formulation, modeling the intracell interference as colored Gaussian noise. This low-complexity detector is especially useful for systems with orthogonal downlink spreading codes, as orthogonality between own cell signals cannot be maintained in a frequency-selective channel. The performance of the proposed receiver is quantified via analysis and simulation for different dispersive channels, including Rayleigh fading channels. Gains on the order of 1–3.5 dB are achieved, depending on the dispersiveness of the channel, with only a modest increase in the number of fingers. For a Wideband CDMA (WCDMA) system and a realistic mobile radio channel, this translates to capacity gains on the order of 100%.**

***Index Terms*—Code division multiple access (CDMA), interference suppression, maximum likelihood detection, multipath channels, spread spectrum communication.**

I. Introduction

As DEMAND for wireless communications continues to grow, third-generation cellular communications systems are being standardized to provide flexible voice and data services. Standardization bodies around the world are developing systems based on direct-sequence code-division multiple-access (DS-CDMA). In North America, the second generation DS-CDMA standard IS-95 is being used as a basis for a third-generation system (IS-2000) with wider bandwidth [2]. In Japan and Europe, a third-generation wideband CDMA (WCDMA) system [1], [2] is also being developed. Currently, there is significant effort to harmonize and merge these systems into a common, global third generation CDMA standard.

From a receiver perspective, a wider bandwidth usually corresponds to a smaller chip period, increasing multipath resolution. In the downlink, where user signals from the same base station pass through the same dispersive channel, increased multipath resolution results in interference with significant spectral distortion. Also, the increased multipath resolution leads to loss of orthogonality to interferers within the cell in systems using orthogonal spreading codes.

The purpose of this paper is to develop a downlink receiver approach that takes advantage of these interference properties. As downlink receivers are typically small, battery powered, portable devices, the simple RAKE receiver structure is used, in which despread values produced by RAKE "fingers" are combined to generate a decision statistic. The interference components of the different RAKE fingers are modeled as colored, Gaussian noise to account for multipath dispersion and pulse shaping. The use of orthogonal spreading codes is accounted for when computing noise correlation between fingers and when determining the noise powers on the different RAKE fingers. These noise properties are used in a maximum likelihood (ML) approach to determine combining weights. Finger placement is based on maximizing the signal-to-noise ratio (SNR) of the decision statistic. By contrast, conventional RAKE reception uses finger placement and combining weights corresponding to the channel impulse response of the signal of interest (see, for example, [3, pp. 797–806]). As the proposed approach uses the RAKE receiver structure, but with possibly different finger placement and combining weights, it can be viewed as a generalized RAKE receiver. We will show results for a realistic mobile radio channel that indicate improvements in capacity on the order of 100% with no increase in the number of fingers and some additional complexity in calculating the combining weights. These gains, for a modest increase in complexity, make the proposed receiver a good candidate for improving downlink performance in both the existing IS-95 system and the forthcoming third-generation CDMA systems.

In the past, other single-user detection methods have been developed which model interference in a similar way. Noneaker [4] proposed a modified RAKE receiver for a downlink CDMA system where the combining is based on the signal-to-interference ratio per finger instead of the signal strength, accounting for uneven noise powers between fingers due to the use of orthogonal spreading codes. However, the color (correlation) between the fingers was not considered.

Modeling interference as colored noise due to the pulse shaping was used in the work by Monk *et al.* [5]–[7], Wong *et al.* [8], [9], and Yoon *et al.* [10], [11]. Monk *et al.* considered frequency nonselective uplink channels with random spreading codes, proposing an approach that exploits the color introduced by the pulse shaping. An alternative structure based on this approach was given by Wong *et al.* [8]. Yoon *et al.* extended

Manuscript received August 1999; revised February 28, 2000.

G. E. Bottomley and Y.-P. E. Wang are with Ericsson Inc., RTP, NC 27709 USA (e-mail: bottoml@rtp.ericsson.se; wang@rtp.ericsson.se).

T. Ottosson is with the Department of Signals and Systems, Chalmers University of Technology, SE-412 96 Göteborg, Sweden (e-mail: tony.ottosson@s2.chalmers.se).

Publisher Item Identifier S 0733-8716(00)06120-5.

this approach to exploit cyclostationarity when the timing information for a few, dominant interferers is available. Wong *et al.* [9] used timing information for all interferers and included coloration due to multipath dispersion in the uplink of a CDMA system.

Coloration introduced by multipath time dispersion in the downlink was considered by Klein [12], [13] and Bottomley [14]. Klein presented a block-based sequence detector for the downlink, based on equalization at the chip level followed by despreading and sequence detection. When orthogonal codes are used, zero-forcing equalization eliminates interference between users in the same cell as well as between symbols. Bottomley used an approach based on the matched filter for colored noise, restricting the solution to a finite impulse response (FIR) filter with a number of taps comparable to the RAKE receiver. As a consequence, finger placement and combining weight design tradeoff matching to the channel and whitening the noise. The approach can be viewed as a RAKE receiver for colored noise, where the primary source of coloration is multipath time dispersion.

In this paper, a generalized RAKE receiver approach is developed for interference suppression and multipath mitigation in the downlink of a DS-CDMA system. This approach can be viewed as a significant extension of the approach in [14], taking into account the use of orthogonal spreading codes, the use of noncontiguous, fractionally spaced, finger placement, and the effects of pulse shaping. Unlike conventional RAKE reception, performance can be improved by increasing the number of RAKE fingers beyond the number of multipath components. Expressions for bit-error rate (BER) are derived for use in evaluating performance and optimizing RAKE finger placement. Link simulation is used to verify the analysis. A semianalytical method is used to evaluate performance in frequency-selective fading channels.

This paper is organized as follows. The system model is described in Section II, followed by the introduction of the generalized RAKE receiver in Section III. Performance is analyzed in Section IV, and both analytical and simulation results are given in Section V. Finally, some concluding remarks and suggestions for future research are given in Section VI.

II. System Model

A complex, baseband equivalent model for a downlink DS-CDMA system is illustrated in Fig. 1. There are K user signals, a desired user (user 0) and $K-1$ multiuser interfering (MUI) signals. The ith data symbol for user k, $s_k(i)$, is spread using the symbol-period-dependent spreading waveform, $a_{k,i}(t)$. Hence, the transmitted signal of user k can be expressed as

$$x_k(t) = \sqrt{E_k} \sum_{i=-\infty}^{\infty} s_k(i) a_{k,i}(t - iT) \tag{1}$$

where E_k is the average symbol energy, and T is the symbol duration. Each data symbol is assumed to have unity amplitude, i.e.,

$$|s_k(i)|^2 = 1. \tag{2}$$

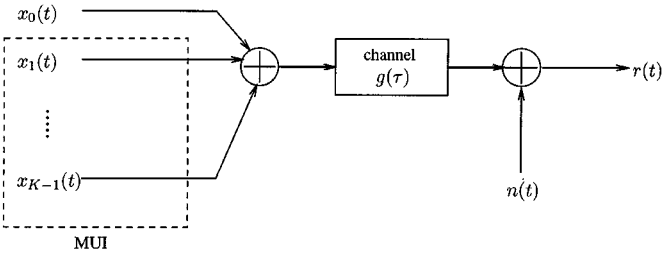

Fig. 1. System model.

The spreading waveform for the kth user and the ith bit consists of a complex chip sequence, $\{c_{k,i}(j)\}_{j=0}^{N-1}$, where N is the spreading factor, convolved with the chip pulse shape, $p(t)$, giving

$$a_{k,i}(t) = \frac{1}{\sqrt{N}} \sum_{j=0}^{N-1} c_{k,i}(j) p(t - jT_c) \tag{3}$$

where T_c is the chip duration. As in most DS-CDMA systems, it is assumed that the spreading code is the product of a user-specific spreading code and a base-station-specific scrambling code. The user-specific spreading codes are assumed to be mutually orthogonal, i.e.,

$$\boldsymbol{c}_{k,i}^H \boldsymbol{c}_{j,i} = 0, \qquad k \neq j \tag{4}$$

where $\boldsymbol{c}_{k,i} = [c_{k,i}(0), c_{k,i}(1), \ldots, c_{k,i}(N-1)]^T$, superscript T denotes transpose, and superscript H denotes Hermitian transpose. For scrambling codes, we assume a complex sequence composed of two random, binary sequences. Thus, assuming the chip values are normalized to have unity amplitude, the chip values $c_{k,i}(j)$ take on the values $\pm 1/\sqrt{2} \pm j/\sqrt{2}$.

Both Nyquist and non-Nyquist pulse shaping are considered. If the pulse shape is Nyquist, then each of the kth user's symbols has energy E_k, and (1) and (2) imply that the spreading waveform is normalized so that $\int_{-\infty}^{\infty} |a_{k,i}(t)|^2 \, dt = 1$. If the pulse shape is not Nyquist, then E_k in (1) is defined to be the *average* symbol energy, and (1) and (2) imply that $E\{\int_{-\infty}^{\infty} |a_{k,i}(t)|^2 \, dt\} = 1$. In either case, the normalization of the spreading waveform and the assumption of unity chip sequence values imply that the pulse shape is normalized so that $\int_{-\infty}^{\infty} |p(t)|^2 \, dt = 1$.

At the base station transmitter, the signals of all K users are symbol synchronously added before passing through a multipath propagation channel characterized by the baseband equivalent impulse response

$$g(\tau) = \sum_{l=0}^{L-1} g_l \delta(\tau - \tau_l) \tag{5}$$

where L is the number of resolvable multipaths, and g_l and τ_l are the complex-valued channel coefficient and the delay for the lth path, respectively. The channel parameters g_l and τ_l are assumed known in the despreading and demodulation process, although in practice the impulse response of the channel is typically estimated using pilot symbols or a pilot channel.

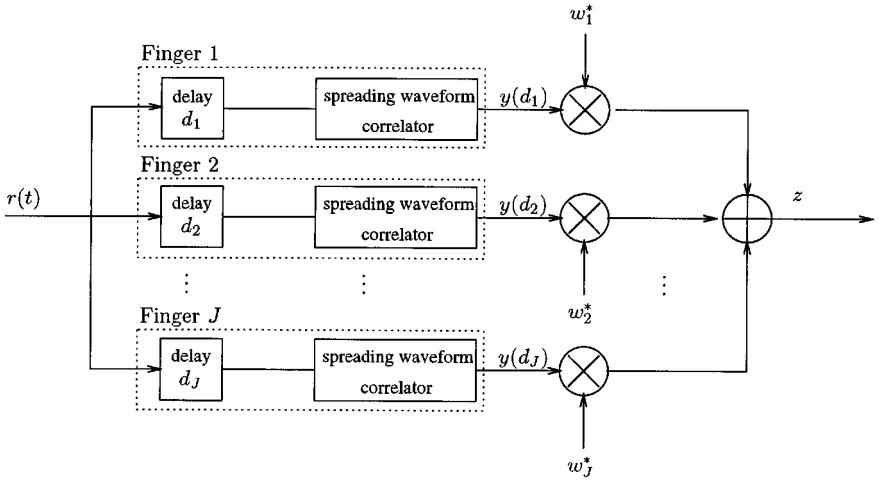

Fig. 2. RAKE receiver structure.

The received signal can be expressed as

$$r(t) = \sum_{l=0}^{L-1} g_l x_0(t-\tau_l) + \sum_{k=1}^{K-1}\sum_{l=0}^{L-1} g_l x_k(t-\tau_l) + n(t) \quad (6)$$

where the noise $n(t)$ models intercell interference and thermal noise, which together are assumed to be white and Gaussian with one-sided power spectral density N_0. The model can readily be modified to take into account also the color of the interference from neighboring base stations. If the mobile receives many base station signals, the intercell interference will be close to white, being mildly colored by the pulse shape, thus justifying the chosen model.

III. The Generalized RAKE Receiver

In this section, the proposed generalized RAKE receiver structure is given. The combining weights are derived from maximum likelihood (ML) principles, and the finger locations are determined based on signal-to-noise ratio (SNR) maximization. We start with the receiver structure.

A. Receiver Structure

We assume a RAKE receiver structure, in a form convenient for analysis. As illustrated in Fig. 2, the structure consists of a bank of J RAKE fingers, each correlating to a different delay of the received signal. The finger outputs are then combined to form a decision statistic. The structure is equivalent to more practical forms, in which the received signal is first filtered with a chip pulse shaping matched filter and despreading is performed using received chip samples and the spreading code sequence.

For a given symbol of interest, e.g., symbol 0 of user 0, the spreading waveform correlator at each finger is used to despread the spread spectrum signal, resulting in the set of despread values $\{y(d_j) = \int_{-\infty}^{\infty} r(t+d_j)a_{0,0}^*(t)\,dt;\ j = 1, 2, \ldots, J\}$. These despread values are combined using combining coefficients $\boldsymbol{w} = [w_1, w_2, \ldots, w_J]^T$ to produce a decision statistic

$$z = \sum_{j=1}^{J} w_j^* y(d_j) = \boldsymbol{w}^H \boldsymbol{y} \quad (7)$$

where $\boldsymbol{y} = [y(d_1), y(d_2), \ldots, y(d_J)]^T$.

Given the decision statistic z, symbol detection then depends on the modulation used. DS-CDMA standards typically employ BPSK or QPSK modulation. For BPSK modulation ($s_0(0) = \pm 1$), the detector is $\hat{s}_0(0) = \text{sgn}(\text{Re}\{z\})$. For QPSK modulation [$s_0(0) = (b_0^I(0) + jb_0^Q(0))/\sqrt{2}$, where $b_0^I(0), b_0^Q(0) \in \{\pm 1\}$], the detectors for the individual bits are $\hat{b}_0^I(0) = \text{sgn}(\text{Re}\{z\})$ and $\hat{b}_0^Q(0) = \text{sgn}(\text{Im}\{z\})$, respectively. Soft bit values can be obtained by omitting the sgn$(\cdot)$ operations.

In the special case of the traditional RAKE receiver, the finger delays would equal the channel delays ($J = L$, and $d_j = \tau_{j-1}$, $j = 1, 2, \ldots, L$) and the weights would be the channel coefficients ($w_j = g_{j-1}$, $j = 1, 2, \ldots, L$). However, we will let the number of fingers, J, the finger delays, $\{d_j\}_{j=1}^J$, and the combining weights, $\{w_j\}_{j=1}^J$, be design parameters. The resulting receiver is referred to as the *generalized RAKE (G-RAKE) receiver* since it has the same structure as the conventional RAKE receiver, but with different delays and weights. Unlike the conventional RAKE receiver, it will be shown that the G-RAKE receiver benefits from using more fingers than the number of multipaths ($J > L$).

B. Combining Weights and Finger Delays

We first focus on the combining weights. The vector of finger outputs can be expressed as

$$\boldsymbol{y} = \boldsymbol{h}s_0(0) + \boldsymbol{u} \quad (8)$$

where $s_0(0)$ is the symbol of interest, $\boldsymbol{h}$ is a vector of complex values corresponding to the symbol of interest, and $\boldsymbol{u}$ models the overall noise (noise and interference). Vector $\boldsymbol{u}$ is assumed to be a vector of complex-valued Gaussian noise with zero mean and covariance $\boldsymbol{R}_u = E[\boldsymbol{u}\boldsymbol{u}^H]$, where $E[\cdot]$ denotes expected value. It can be shown (see, e.g., [15, pp. 478–479]) that the maximum likelihood (ML) detector for $s_0(0)$ given the observation vector $\boldsymbol{y}$ depends only on the decision statistic given in (7) with combining weights

$$\boldsymbol{w} = \boldsymbol{R}_u^{-1}\boldsymbol{h}. \quad (9)$$

It should also be observed that the model of (8) does not introduce an extra level of approximation since we already have as-

sumed that the intracell interference can be modeled as colored Gaussian noise, and that thermal noise and intercell interference can be modeled as white Gaussian noise.

Using the system model given in Section II, expressions for $\boldsymbol{R}_u$ and $\boldsymbol{h}$ are derived. The despread value $y(d_j)$ can be viewed as a sample at the output of a time-continuous spreading waveform matched filter, whose output $y(t)$ is given by

$$\begin{aligned} y(t) &= \int_{-\infty}^{\infty} r(\tau) a_{0,0}^*(\tau - t)\, d\tau \\ &= \sum_{k=0}^{K-1} \sum_{l=0}^{L-1} \sum_{i=-\infty}^{\infty} \sqrt{E_k}\, g_l s_k(i) R_{k,i}(t - iT - \tau_l) + \tilde{n}(t). \end{aligned} \tag{10}$$

Here $\tilde{n}(t)$ is the noise component after filtering, and $R_{k,i}(t)$ is the cross-correlation function between the waveforms of the ith symbol of user k and the 0th symbol of user 0, i.e.,

$$R_{k,i}(t) \triangleq \int_{-\infty}^{\infty} a_{k,i}(t+\tau) a_{0,0}^*(\tau)\, d\tau. \tag{11}$$

Expanding (11) using (3) gives

$$R_{k,i}(t) = \frac{1}{N} \sum_{l=0}^{N-1} \sum_{m=0}^{N-1} c_{k,i}(l) c_{0,0}^*(m) R_p(t - (l-m)T_c) \tag{12}$$

where $R_p(t) \triangleq \int_{-\infty}^{\infty} p(t+\tau) p^*(\tau)\, d\tau$ is the autocorrelation of the chip pulse shape.

The waveform cross-correlation function can be expressed in terms of the standard aperiodic correlation function $C_{k,i}(m)$ defined in [16], i.e.,

$$C_{k,i}(m) \triangleq \begin{cases} \displaystyle\sum_{n=0}^{N-1-m} c_{k,i}(n) c_{0,0}^*(n+m), & 0 \le m \le N-1 \\ \displaystyle\sum_{n=0}^{N-1+m} c_{k,i}(n-m) c_{0,0}^*(n), & 1-N \le m < 0. \end{cases} \tag{13}$$

As a result, (12) reduces to

$$R_{k,i}(t) = \frac{1}{N} \sum_{m=1-N}^{N-1} C_{k,i}(m) R_p(t + mT_c) \tag{14}$$

which can be interpreted as a discrete-time convolution of the code aperiodic correlation function with the pulse shape autocorrelation function. Note that $C_{k,0}(0) = 0$, $k \neq 0$, due to the orthogonality between downlink signals, and $C_{0,0}(0) = N$.

The autocorrelation function of the filtered noise, $\tilde{n}(t)$, is given by

$$\begin{aligned} R_{\tilde{n}}(t_1, t_2) &\triangleq E[\tilde{n}(t_1)\tilde{n}^*(t_2)] \\ &= N_0 R_{0,0}(t_1 - t_2) \\ &= \frac{N_0}{N} \sum_{m=1-N}^{N-1} C_{0,0}(m) R_p(t_1 - t_2 + mT_c). \end{aligned} \tag{15}$$

From (10), the matched filter output can be split into four terms: the desired component $y_d(t)$, the self interference component $y_{\mathrm{ISI}}(t)$, the multiuser interference component $y_{\mathrm{MUI}}(t)$, and the noise component $n'(t)$. That is

$$\begin{aligned} y(t) = \sqrt{E_0}\, y_d(t) s_0(0) + \sqrt{E_0}\, y_{\mathrm{ISI}}(t) + \sqrt{E_I}\, y_{\mathrm{MUI}}(t) \\ + \sqrt{N_0}\, n'(t) \end{aligned} \tag{16}$$

where

$$y_d(t) = \sum_{l=0}^{L-1} g_l R_{0,0}(t - \tau_l) \tag{17}$$

$$y_{\mathrm{ISI}}(t) = \sum_{l=0}^{L-1} \sum_{\substack{i=-\infty \\ i \neq 0}}^{\infty} g_l s_0(i) R_{0,i}(t - iT - \tau_l) \tag{18}$$

$$\begin{aligned} y_{\mathrm{MUI}}(t) = \frac{1}{\sqrt{E_I}} \sum_{k=1}^{K-1} \sqrt{E_k} \sum_{l=0}^{L-1} \sum_{i=-\infty}^{\infty} g_l s_k(i) \\ \cdot R_{k,i}(t - iT - \tau_l) \end{aligned} \tag{19}$$

and $E_I \triangleq \sum_{k=1}^{K-1} E_k$ is the total symbol energy of the intracell interference.

Sampling the matched filter output at delays $(d_1, \ldots, d_J)$ gives $\boldsymbol{y} = [y(d_1), \ldots, y(d_J)]^T$. From (16), $\boldsymbol{y}$ can be expressed as

$$\boldsymbol{y} = \sqrt{E_0}\, \boldsymbol{y}_d s_0(0) + \sqrt{E_0}\, \boldsymbol{y}_{\mathrm{ISI}} + \sqrt{E_I}\, \boldsymbol{y}_{\mathrm{MUI}} + \sqrt{N_0}\, \boldsymbol{n}' \tag{20}$$

where $\boldsymbol{y}_d = [y_d(d_1), y_d(d_2), \ldots, y_d(d_J)]^T$, $\boldsymbol{y}_{\mathrm{ISI}} = [y_{\mathrm{ISI}}(d_1), y_{\mathrm{ISI}}(d_2), \ldots, y_{\mathrm{ISI}}(d_J)]^T$, $\boldsymbol{y}_{\mathrm{MUI}} = [y_{\mathrm{MUI}}(d_1), y_{\mathrm{MUI}}(d_2), \ldots, y_{\mathrm{MUI}}(d_J)]^T$, and $\boldsymbol{n}' = [n'(d_1), n'(d_2), \ldots, n'(d_J)]^T$.

Observe that (20) has the form of (8), in which

$$\boldsymbol{h} = \sqrt{E_0}\, \boldsymbol{y}_d \tag{21}$$

and $\boldsymbol{u} = \sqrt{E_0}\, \boldsymbol{y}_{\mathrm{ISI}} + \sqrt{E_I}\, \boldsymbol{y}_{\mathrm{MUI}} + \sqrt{N_0}\, \boldsymbol{n}'$. Assuming $\boldsymbol{y}_{\mathrm{ISI}}$, $\boldsymbol{y}_{\mathrm{MUI}}$, and $\boldsymbol{n}'$ are uncorrelated

$$\boldsymbol{R}_u = E_0 \boldsymbol{R}_{\mathrm{ISI}} + E_I \boldsymbol{R}_{\mathrm{MUI}} + N_0 \boldsymbol{R}_{n'} \tag{22}$$

where $\boldsymbol{R}_{\mathrm{ISI}} = E[\boldsymbol{y}_{\mathrm{ISI}} \boldsymbol{y}_{\mathrm{ISI}}^H]$, $\boldsymbol{R}_{\mathrm{MUI}} = E[\boldsymbol{y}_{\mathrm{MUI}} \boldsymbol{y}_{\mathrm{MUI}}^H]$, and $\boldsymbol{R}_{n'} = E[\boldsymbol{n}' \boldsymbol{n}'^H]$. In forming these covariance matrices, the expectation for $\boldsymbol{R}_{\mathrm{MUI}}$ is over the interferers' symbols and spreading codes, while the expectation in $\boldsymbol{R}_{\mathrm{ISI}}$ is over the desired signal's previous and future symbols and spreading codes. Strictly speaking, the desired signal's previous and future symbol spreading codes are known and could be used in computing $\boldsymbol{R}_{\mathrm{ISI}}$. However, this knowledge is not used here as its benefit is considered small, and such knowledge may be difficult to use in a practical implementation.

Thus, it suffices to average over the aperiodic cross-correlation function $C_{k,i}(m)$ given in (13). It can be easily shown that for the assumed spreading sequences (complex random scrambling sequences and orthogonal user-specific spreading sequences)

$$E[C_{k,i}(m) C_{k,i}^*(n)] = 0, \qquad m \neq n \tag{23}$$

$$E[|C_{k,i}(m)|^2] = \begin{cases} 0, & i = m = 0,\ k \neq 0 \\ N^2, & i = m = k = 0 \\ N - |m|, & \text{otherwise.} \end{cases} \tag{24}$$

Using (23) and (24), the elements in the matrices $\boldsymbol{R}_{\mathrm{ISI}}$ and $\boldsymbol{R}_{\mathrm{MUI}}$ can be computed. For example

$$\begin{aligned} R_{\mathrm{ISI}}(d_1, d_2) &= E[y_{\mathrm{ISI}}(d_1) y^*_{\mathrm{ISI}}(d_2)] \\ &= \sum_{l=0}^{L-1} \sum_{q=0}^{L-1} \sum_{\substack{i=-\infty \\ i\neq 0}}^{\infty} g_l g_q^* E[R_{0,i}(d_1 - iT - \tau_l) \\ &\quad \times R^*_{0,i}(d_2 - iT - \tau_q)] \\ &= \frac{1}{N^2} \sum_{l=0}^{L-1} \sum_{q=0}^{L-1} \sum_{\substack{i=-\infty \\ i\neq 0}}^{\infty} g_l g_q^* \sum_{m=1-N}^{N-1} (N - |m|) \\ &\quad \times R_p(d_1 + mT_c - iN - \tau_l) \\ &\quad \times R_p^*(d_2 + mT_c - iN - \tau_q). \end{aligned} \tag{25}$$

Similarly, we have

$$\begin{aligned} R_{\mathrm{MUI}}(d_1, d_2) &= E[y_{\mathrm{MUI}}(d_1) y^*_{\mathrm{MUI}}(d_2)] \\ &= \frac{1}{N^2} \sum_{l=0}^{L-1} \sum_{q=0}^{L-1} g_l g_q^* \sum_{i=-\infty}^{\infty} \sum_{m=1-N}^{N-1} (N - |m|) \\ &\quad \times R_p(d_1 + mT_c - iT - \tau_l) \\ &\quad \times R_p^*(d_2 + mT_c - iT - \tau_q)(1 - \delta(m)\delta(i)). \end{aligned} \tag{26}$$

Furthermore

$$\begin{aligned} R_{n'}(d_1, d_2) &= E[n'(d_1)(n'(d_2))^*] \\ &= R_{0,0}(d_1 - d_2) \\ &= \frac{1}{N} \sum_{m=1-N}^{N-1} C_{0,0}(m) R_p(d_1 - d_2 + mT_c). \end{aligned} \tag{27}$$

Finally, from (17), we have

$$y_d(d_1) = \frac{1}{N} \sum_{l=0}^{L-1} g_l \sum_{m=1-N}^{N-1} C_{0,0}(m) R_p(d_1 + mT_c - \tau_l). \tag{28}$$

Elements corresponding to the other delay combinations, can easily be obtained by replacing d_1 and d_2 in the above equations by the appropriate delays.

Note that $y_d(d_1)$ and $R_{n'}(d_1, d_2)$ are functions of the desired signal's code aperiodic autocorrelation function $\boldsymbol{C} \triangleq \{C_{0,0}(m)\}_{m=1-N}^{N-1}$, which changes from symbol to symbol. In practice, it is cumbersome to vary the weights corresponding to the varying aperiodic autocorrelation function. Instead, one can design the weights using the *average* aperiodic autocorrelation function

$$\overline{C}_{0,0}(m) \triangleq E[C_{0,0}(m)] = N\delta(m). \tag{29}$$

Replacing $C_{0,0}(m)$ in (28) and (27) with $\overline{C}_{0,0}(m)$ from (29) gives

$$\overline{y}_d(d_1) = \sum_{l=0}^{L-1} g_l R_p(d_1 - \tau_l) \tag{30}$$

$$\overline{R}_{n'}(d_1, d_2) = R_p(d_1 - d_2) \tag{31}$$

which can be used to develop autocorrelation-independent weights.

Choosing the finger delays is a tradeoff between matching to the channel and whitening the noise. We propose using a set of J finger delays that optimizes a specific performance criterion. For a time-invariant channel, maximization of the signal-to-noise ratio (SNR) of the decision statistic z is used. For a time-varying channel, either maximization of the instantaneous SNR or minimization of the BER, averaged over the fading channel coefficients, is used. A suitable choice for J is $J \leq 2L$ fingers as indicated by the numerical results in Section V.

Unlike the combining weights, there is no closed form expression for such delays. As a result, we search a window of potential delays and find the set that optimizes the performance criterion. The window spans from several chip periods before the earliest arriving multipath component to several chip periods after the latest arriving multipath component. The example that follows suggests a simpler strategy, in which L fingers are positioned on the multipath components (to collect energy) and the remaining $J - L$ fingers are placed based on the strongest taps of the inverse channel filter (to suppress interference).

C. Example

A simple example is used to illustrate the proposed approach. Consider a two-ray, chip-spaced channel and two CDMA signals. Ignoring adjacent symbol periods, the received signal $r(t)$ during one symbol period is given by

$$\begin{aligned} r(t) = g_0(S_s a_s(t) + S_i a_i(t)) + g_1(S_s a_s(t - T_c) \\ + S_i a_i(t - T_c)) \end{aligned} \tag{32}$$

where g_0 and g_1 are the channel coefficients, S_s and S_i are the desired and interferer's symbol values ($|S_s|^2 = |S_i|^2 = 1$), and $a_s(t)$ and $a_i(t)$ are the spreading waveforms for the desired signal and interferer, respectively.

Assuming despreading every chip period and that the pulses are normalized Nyquist pulses, the despread values are given by

$$\begin{aligned} y(mT_c) &= \int_{-\infty}^{\infty} a_s^*(t) r(t + mT_c)\, dt \\ &= \frac{1}{\sqrt{N}} \sum_{j=0}^{N-1} c_s^*(j) \tilde{r}(j + m) \end{aligned} \tag{33}$$

where $c_s(j)$ is the desired signal's chip sequence and $\tilde{r}(j)$ is a discrete-time signal obtained by filtering the received signal with a filter matched to the chip pulse shape, i.e., $\tilde{r}(j) = \int_{-\infty}^{\infty} r(t) p^*(t - jT_c)\, dt$. From (3) and (32), $\tilde{r}(j)$ can be expressed as

$$\begin{aligned} \tilde{r}(j) &= \frac{g_0}{\sqrt{N}} (S_s c_s(j) + S_i c_i(j)) \\ &\quad + \frac{g_1}{\sqrt{N}} (S_s c_s(j-1) + S_i c_i(j-1)) \end{aligned} \tag{34}$$

where $c_i(j)$ is the interferer's chip sequence.

A conventional RAKE receiver would combine $y(0)$ and $y(T_c)$ according to (7), using the weight vector $\boldsymbol{w} = [g_0, g_1]^T$. However, with the G-RAKE approach, the statistical properties of the interference component would also be used. The interference component of $y(mT_c)$ is obtained by substituting the interference component of $\tilde{r}(j)$ from (34) into (33), giving

$$y_i(mT_c) = \frac{g_0}{N} S_i C_i(-m) + \frac{g_1}{N} S_i C_i(1-m) \tag{35}$$

where $C_i(m)$ is the aperiodic cross-correlation between the chip sequences [see (13)]. With orthogonal codes, $C_i(0) = 0$, so that

$$y_i(-T_c) = \frac{g_0}{N} S_i C_i(1) + \frac{g_1}{N} S_i C_i(2) \tag{36}$$

$$y_i(0) = \frac{g_1}{N} S_i C_i(1) \tag{37}$$

$$y_i(T_c) = \frac{g_0}{N} S_i C_i(-1). \tag{38}$$

With random scrambling, these $C_i(m)$ terms can be modeled as uncorrelated random variables with roughly equal power of N (assuming large N).

First, consider placing fingers according to a conventional RAKE receiver, at lags $m = 0$ and $m = 1$. From (37) and (38), the impairment correlation matrix is given by

$$\boldsymbol{R} = \begin{bmatrix} |g_1|^2 & 0 \\ 0 & |g_0|^2 \end{bmatrix}. \tag{39}$$

Assuming $|g_0|^2 > |g_1|^2$, there is more interference power on the second finger output. This is reflected in the resulting weights, $\boldsymbol{w} = [g_0/|g_1|^2, g_1/|g_0|^2]^T$. Thus, $y(T_c)$ is weighted less because of more interference power.

Second, consider placing a third finger at lag $m = -1$. From (36) and (38), the impairment correlation matrix is given by

$$\boldsymbol{R} = \begin{bmatrix} |g_0|^2 + |g_1|^2 & g_0 g_1^* & 0 \\ g_0^* g_1 & |g_1|^2 & 0 \\ 0 & 0 & |g_0|^2 \end{bmatrix}. \tag{40}$$

Observe that, in this case, there are nonzero off-diagonal elements, indicating correlation between interference values. (Off-diagonal elements would have occurred in the previous case if the codes had not been orthogonal.) The resulting weights are given by

$$\boldsymbol{w} = \boldsymbol{R}^{-1} \begin{bmatrix} 0 \\ g_0 \\ g_1 \end{bmatrix} = \frac{1}{D} \begin{bmatrix} -|g_0|^2 g_0^2 g_1^* \\ |g_0|^2(|g_0|^2 + |g_1|^2) g_0 \\ |g_1|^4 g_1 \end{bmatrix} \tag{41}$$

where $D = |g_0|^2|g_1|^4$ and $1/D$ is a common scaling factor that can be omitted. Observe that even though the channel coefficient at lag $m = -1$ is zero, the corresponding combining weight is nonzero (unlike conventional RAKE), due to the off-diagonal elements in $\boldsymbol{R}$.

The suppression of interference can be seen by applying the weights (scaling factor omitted) to the interference components of $y(mT_c)$, giving

$$\begin{aligned} z_i =& -|g_0|^2 (g_0^*)^2 g_1 \left(\frac{g_0}{N} S_i C_i(1) + \frac{g_1}{N} S_i C_i(2) \right) \\ &+ |g_0|^2 (|g_0|^2 + |g_1|^2) g_0^* \frac{g_1}{N} S_i C_i(1) \\ &+ |g_1|^4 g_1^* \frac{g_0}{N} S_i C_i(-1) \\ =& \left\{ -|g_0|^2 (g_0^*)^2 g_1^2 C_i(2) + [-|g_0|^4 g_0^* g_1 + |g_0|^4 g_0^* g_1 \right. \\ &\left. + |g_0|^2 |g_1|^2 g_0^* g_1] C_i(1) + |g_1|^4 g_1^* g_0 C_i(-1) \right\} \frac{S_i}{N}. \end{aligned} \tag{42}$$

Observe that the first two terms in brackets cancel, so that including $y(-T_c)$ in the combining process leads to partial cancellation of the interference.

The placement of the extra finger just before the first, largest ray, also has an inverse channel filtering interpretation. In [14], it was shown that when own-cell interference dominates, the receiver tries to approximate an inverse channel filter (undoing the noise coloration caused by the channel). Using the stability criterion, the inverse channel filter for the example above would have taps at delays of $m = 0, -1, -2, \ldots$. Thus, placing the extra finger at $m = -1$ allows the G-RAKE approach to approximate inverse channel filtering.

IV. Performance Analysis

The standard Gaussian approximation regarding interference is used with a SNR analysis to derive the BER for BPSK and QPSK modulation. Further approximations are made to average the effects of the random scrambling sequences used in the spreading process.

Given a specific weight vector $\boldsymbol{w}$, the symbol SNR ratio at the output of the combiner (the decision statistic z) can easily be shown to be

$$\text{SNR} = \frac{\boldsymbol{w}^H \boldsymbol{h} \boldsymbol{h}^H \boldsymbol{w}}{\boldsymbol{w}^H \boldsymbol{R}_u \boldsymbol{w}}. \tag{43}$$

For the G-RAKE receiver, the weights are given in (9) and the resulting signal-to-noise ratio, using (21) and (22), is

$$\begin{aligned} &\text{SNR}(\boldsymbol{C}) \\ &\quad = E_0 \boldsymbol{y}_d^H \boldsymbol{R}_u^{-1} \boldsymbol{y}_d \\ &\quad = \boldsymbol{y}_d^H \left\{ \boldsymbol{R}_{\text{ISI}} + \left(\frac{E_0}{E_I} \right)^{-1} \boldsymbol{R}_{\text{MUI}} + \left(\frac{E_0}{N_0} \right)^{-1} \boldsymbol{R}_{n'} \right\}^{-1} \boldsymbol{y}_d \end{aligned} \tag{44}$$

where $\boldsymbol{C}$ is the desired signal's code aperiodic autocorrelation function as defined in the previous section. It should also be noted that the SNR given in the above equations is the ratio between the *symbol* energy and the power spectral density of the overall noise. As a result, the BER can be expressed as

$$P_e(\boldsymbol{C}) = \tfrac{1}{2} \operatorname{erfc}\left(\sqrt{\alpha \text{SNR}(\boldsymbol{C})} \right) \tag{45}$$

where α is the factor for converting symbol energy to bit energy, i.e., $\alpha = 1$ for BPSK, and $\alpha = 1/2$ for QPSK. Taking the expected value over the desired signal's spreading code (that is, the aperiodic autocorrelation function) and using Jensen's inequality gives

$$E[P_e(\boldsymbol{C})] \geq \tfrac{1}{2}\,\mathrm{erfc}\left(\sqrt{E[\alpha \mathrm{SNR}(\boldsymbol{C})]}\right) \approx \tfrac{1}{2}\,\mathrm{erfc}\left(\sqrt{\alpha \mathrm{SNR}(E[\boldsymbol{C}])}\right) \quad (46)$$

so that the average BER is approximately

$$P_e \approx \tfrac{1}{2}\,\mathrm{erfc}\left(\sqrt{\alpha \mathrm{SNR}(E[\boldsymbol{C}])}\right) \quad (47)$$

where $E[\boldsymbol{C}]$ is determined from (29). Equation (47) is an accurate approximation when the $\mathrm{SNR}(\boldsymbol{C})$ variation with $\boldsymbol{C}$ is small enough so that the $\mathrm{erfc}(\cdot)$ function can be well approximated with a linear function. Otherwise, (47) tends to be optimistic. The variation of $\boldsymbol{C}$ depends primarily on the spreading factor N. We found that with typical spreading factors for speech communications ($N = 64$ or 128), the approximation is quite accurate.

For comparison purposes, a similar analysis is performed for the conventional RAKE receiver. For this case, the weight vector corresponds to the multipath coefficients. The BER is then obtained using (43) and (47).

V. Numerical Results

In this section, the analytical results of Section V are used to investigate the properties and potential gains of the generalized RAKE receiver. We start with addressing the accuracy of the analysis by comparison with simulations. The analysis is then used to investigate the performance gain as a function of the channel impulse response and the number of RAKE fingers. Finally, we present semianalytical results for Rayleigh fading channels.

All results given in this section are for a downlink consisting of $K = 24$ user signals transmitted from a single base station, received in the presence of additive white Gaussian noise (AWGN). The composite spreading codes consist of orthogonal Walsh–Hadamard codes of length $N = 128$, followed by a common random complex scrambling code that changes every symbol period. QPSK modulation with root-raised-cosine (RRC) pulse shaping is used with 22% rolloff (as in WCDMA [1]). Knowledge of the multipath channel response is assumed throughout. The autocorrelation-independent weight calculation is used for the G-RAKE receiver.

A. Verification of Analytical Results

First, the performance analysis for the RAKE and G-RAKE receivers was verified via simulation. A representative result is shown in Fig. 3, in which E_b is the energy-per-bit. The channel was assumed to be time-invariant with four paths separated by one chip, relative amplitudes 0, -1.5, -3, and -4.5 dB, and relative phases 0°, 60°, 120°, and 180°. In the simulation, the channel was normalized to give unity power gain. The simulation program generated 2000 realizations of 100 bits each, giving a total of 2×10^5 bits. At the receiver, the conventional RAKE and the G-RAKE approaches were considered. For the conventional RAKE receiver, fingers were placed on all rays. For the G-RAKE receiver, nominal (not necessarily optimized) finger locations were selected, and the analytical expressions were used to determine the optimal combining weights as well as the expected performance. For the G-RAKE receiver, results are shown for: a) 4 fingers positioned at 0, 1, 2, and 3 chip periods (aligned with the paths); b) 4 fingers positioned at -1, 0, 1, and 2 chip periods; and c) 5 fingers at -1, 0, 1, 2, and 3 chip periods.

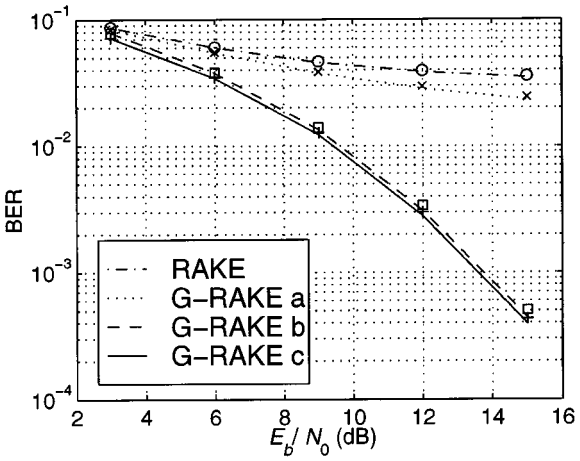

Fig. 3. Comparison of link simulation (markers) and analysis (lines) of the conventional RAKE receiver and the generalized RAKE (G-RAKE) receiver. The channel is a four path chip-spaced channel with relative amplitudes 0, -1.5, -3, and -4.5 dB, and relative phases 0, 60, 120, and 180°. For the G-RAKE receiver, the finger delays are: a) 4 fingers positioned at 0, 1, 2, and 3 chip periods (aligned with the paths); b) 4 fingers positioned at -1, 0, 1, and 2 chip periods; and c) 5 fingers at -1, 0, 1, 2, and 3 chip periods.

Overall, the analytical results accurately predict the simulation results. Most of the analytical results are slightly optimistic, as predicted in Section IV. Although not shown, we have compared analytical results with simulation results for a variety of ray positions (e.g., not chip-spaced), amplitudes and angles. All results showed good agreement between analysis and simulation. We will therefore, in the following, rely on analytical results.

The results in Fig. 3 also provide a convenient example for highlighting the features of the G-RAKE approach. In Case a, the G-RAKE approach places fingers corresponding to the multipath delays, similar to the RAKE approach. A modest gain is achieved, due to the fact that the G-RAKE accounts for the differing "noise" levels on the fingers, as well as noise correlation between fingers. In Case b, the finger placed on the weakest ray is moved to a position just before the first, strongest ray. Performance improves further, demonstrating the tradeoff between collecting signal energy and performing noise whitening. Finally, in Case c, 5 fingers are used, placing 4 corresponding to the multipath delays then placing a fifth finger just before the first, strongest finger. Observe that, contrary to the conventional RAKE approach, performance improves by placing this additional finger at a delay corresponding to no multipath component. Performance improves because the noise on the added finger is correlated to the noise on the remaining fingers, allowing partial cancellation of the overall noise.

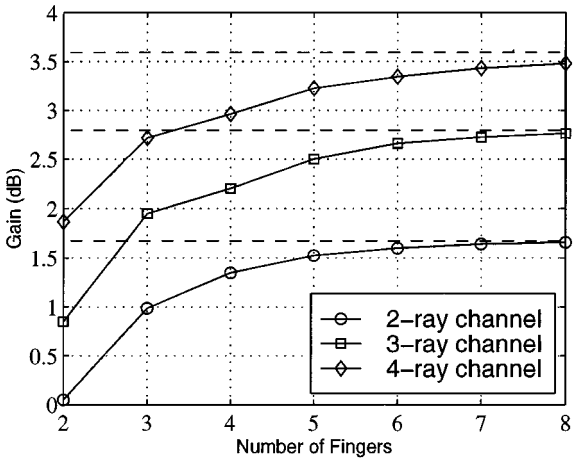

Fig. 4. Gain in signal-to-noise ratio for the G-RAKE receiver compared to the L-finger RAKE receiver for $L = 2$-, 3-, and 4-ray channels. The 4-ray channel is chip spaced, with relative amplitudes of 0, -1.5, -3, and -4.5 dB, and relative phases of 0, 60, 120, and 180°. The 2-ray and 3-ray channels use the first two and three rays, respectively, of the 4-ray channel. The dashed lines are approximate maximum gains for the G-RAKE receivers. $E_b/N_0 = 10$ dB for all users.

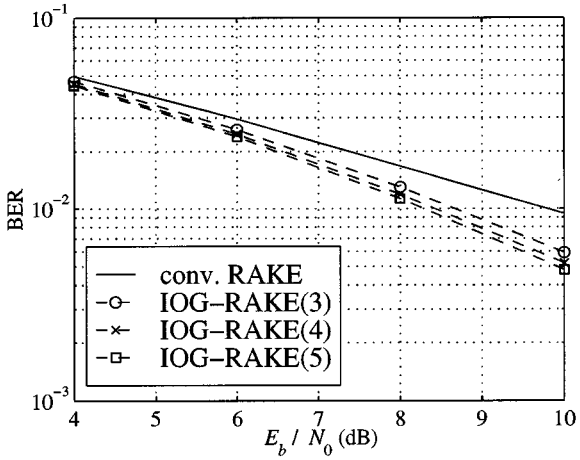

Fig. 5. BER for the RAKE and IOG-RAKE receivers for a 3-ray chip spaced channel with average relative amplitudes of 0, -1.5, and -3 dB. All the rays are independent and Rayleigh fading. The IOG-RAKE receiver has either 3, 4, or 5 fingers and are denoted by IOG-RAKE(3), IOG-RAKE(4), and IOG-RAKE(5), respectively.

B. Performance for Fixed-Coefficient Channels

Next we examine how the performance changes with the number of rays in the channel and the number of fingers in the G-RAKE receiver. To study this, we consider L-ray frequency-selective channels, where $L = 2, 3, 4$. The 4-ray channel response is chip-spaced, with relative amplitudes of 0, -1.5, -3, and -4.5 dB, and relative phases of 0, 60, 120, and 180 degrees. The 2-ray and 3-ray channel responses use the first two and three rays, respectively, of the 4-ray channel. Finger positions for the G-RAKE are optimized assuming that the fingers are within the time window $[\tau_0 - 4T_c, \tau_{L-1} + 4T_c]$ and on a $T_c/2$-spaced grid. The signal-to-noise ratio per bit, E_b/N_0, is 10 dB for all users.

Results in terms of the SNR gain of the G-RAKE compared to the L-finger conventional RAKE are given in Fig. 4. For reference purposes, the gain of using 129 fingers within a window of $[-32T_c, 32T_c]$ on the $T_c/2$-spaced grid is shown (dashed lines) as an approximation to the maximum gain achievable by the G-RAKE receiver. Observe that the gain of the G-RAKE receiver increases with both the number of rays in the channel and the number of fingers. It is also shown that most of the achievable gain, on the order of 1.5–3.5 dB, is obtained using about twice as many fingers as there are channel rays. Thus, $J \approx 2L$ is a reasonable design rule. It is also interesting to see that the G-RAKE receivers with fewer fingers ($J < L$) can perform better than the RAKE receivers. For example, for the 4-ray channel, both the 2- and 3-finger G-RAKE receivers perform better than the 4-finger conventional RAKE receiver. Moreover, the gain will increase with higher load (increased number of users).

C. Performance for Fading Channels

In a typical multipath propagation channel, each of the rays usually experiences Rayleigh fading. Ideally, the finger positions and weights should change with the fading. To study this further, we introduce the concept of an *instantaneous optimum G-RAKE (IOG-RAKE) receiver,* where the receiver finds the optimum finger positions and weights for each realization of the fading channel response. To obtain semianalytical performance results for the fading channel, we averaged the analytical expressions for BER over the fading using Monte-Carlo simulation.

In Fig. 5, results are shown for a 3-ray chip-spaced channel with the average amplitudes of 0, -1.5, and -3 dB. Each of the rays is modeled as having uncorrelated Rayleigh-distributed amplitudes with uncorrelated uniformly distributed phases. The IOG-RAKE receiver has either 3, 4, or 5 fingers, denoted by IOG-RAKE(3), IOG-RAKE(4), and IOG-RAKE(5), respectively. At a nominal BER of 10^{-2}, the gain achieved by the IOG-RAKE receivers compared to the RAKE receiver is 1.2–1.7 dB, depending on the number of fingers. The gain is not as large for the fading case as for the fixed channel case because the rays fade some part of the time, resulting in fewer effective rays. With fewer effective rays, the gains with respect to the RAKE are lower (compare to Fig. 4).

One could argue that the instantaneous optimum G-RAKE is less practical, since the finger positions and the weights need to be reoptimized as the fading changes. A more practical solution would be to fix the positions of the fingers but still allow the combining weights to change with the fading channel coefficients. Thus, instead of finding the instantaneously best finger positions, we are interested in finding a set of fixed finger positions that minimizes the BER. This receiver is referred to as the *average optimum G-RAKE (AOG-RAKE) receiver.* A comparison between the IOG-RAKE and the AOG-RAKE receivers is shown in Fig. 6 for a 5-ray half-chip-spaced fading channel with average amplitudes of 0, -1, -2, -3, and -4 dB. Observe that the small performance difference between the IOG-RAKE and the AOG-RAKE justifies this reduction in complexity.

As a final result, we studied the capacity benefit of using the IOG-RAKE and AOG-RAKE receivers for a realistic mobile radio channel. The channel is the modified ITU vehicular channel model given in [17] with 8 rays of delays 0, 1, 2, 3, 4, 5, 6, and 7 chip periods, and average powers 0.0, -2.4, -6.5, -9.4, -12.7, -13.3, -15.4, and -25.4 dB. BER results as a function

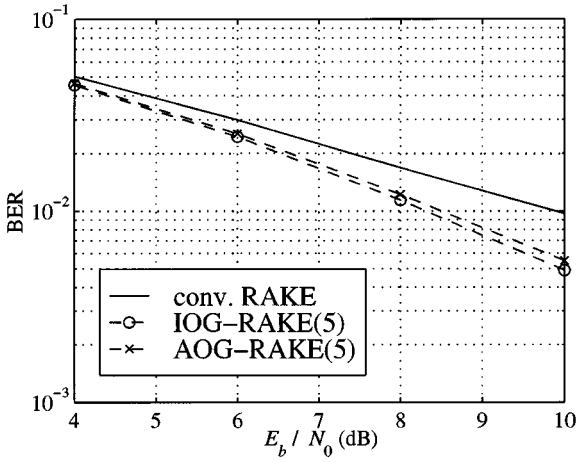

Fig. 6. BER for the RAKE, IOG-RAKE, and AOG-RAKE receivers for a 5-ray half-chip-spaced channel with average relative amplitudes of 0, -1, -2, -3, and -4 dB. All the rays are independent and Rayleigh fading. All receivers have 5 fingers.

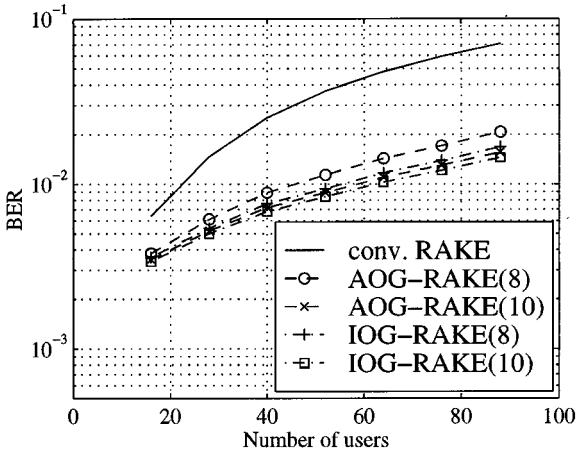

Fig. 7. BER for the RAKE, the IOG-RAKE, and the AOG-RAKE receivers as a function of the number of users K. The channel is an 8-ray vehicular channel with delays 0, 1, 2, 3, 4, 5, 6, and 7 chip periods, and average powers 0.0, -2.4, -6.5, -9.4, -12.7, -13.3, -15.4, and -25.4 dB. All the rays are independent and Rayleigh fading. The G-RAKE receivers have 8 or 10 fingers. $E_b/N_0 = 10$ dB for all users.

of the number of users are shown in Fig. 7. The G-RAKE receivers use 8 or 10 fingers, whereas the RAKE receiver uses 8 fingers. The signal-to-noise ratio for all users is $E_b/N_0 = 10$ dB. The search window is restricted to $[-3T_c, 10T_c]$ on a T_c-spaced grid. Observe that the number of users supported at a BER of 10^{-2} increases from 22 for the RAKE receiver to 45 for the AOG-RAKE receiver with 8 fingers, which is a capacity increase of about 100%. It is furthermore seen that the 8-finger IOG-RAKE and the 10-finger G-RAKE receivers increase capacity by more than 145%. Thus, the G-RAKE receiver can provide significant capacity gains in frequency-selective fading channels, at the expense of a moderate increase in complexity. It is also seen that the gain in capacity increases when the comparison is made at higher BER.

VI. Conclusion

A generalized RAKE receiver is proposed for suppressing own cell interference in the downlink of a DS-CDMA system employing orthogonal codes. The proposed receiver uses the fact that a dispersive channel distorts the interference spectrum and treats this interference as colored noise. Further noise coloration is introduced by the chip pulse shape. Compared to conventional RAKE reception, performance gains are significant (1–3.5 dB in SNR), and performance improves when increasing the number of fingers beyond the number of resolvable multipaths. Most of the potential gain is achieved using twice as many fingers as channel delays. Significant performance gains and a modest increase in complexity make the G-RAKE approach an attractive downlink receiver solution for both second and third generation CDMA systems.

While the focus has been on orthogonal spreading codes and suppressing own cell interference, it is straightforward to extend the results to the use of nonorthogonal codes and to suppressing other cell interference. Of particular interest is the soft handoff scenario, in which interfering users employ a mixture of orthogonal and nonorthogonal codes, and there are two dispersive channels to consider. Future research is needed to quantify performance gains for this case.

Acknowledgment

The authors gratefully acknowledge P. Dent for his significant contributions in the early stages of this work, as well as A. Khayrallah, J.-C. Guey, and the anonymous reviewers of this paper for their helpful comments.

References

[1] E. Dahlman, P. Beming, J. Knutsson, F. Ovesjö, M. Persson, and C. Roobol, "WCDMA—The radio interface for future mobile multimedia communications," *IEEE Trans. Veh. Technol.*, vol. 47, pp. 1105–1118, Nov. 1998.

[2] T. Ojanperä and R. Prasad, "An overview of air interface multiple access for IMT-2000/UMTS," *IEEE Commun. Mag.*, vol. 36, pp. 82–95, Sept. 1998.

[3] J. G. Proakis, *Digital Communications*. New York: McGraw-Hill, 1995.

[4] D. L. Noneaker, "Optimal combining for Rake reception in mobile cellular CDMA forward links," in *Proc. IEEE Military Commun. Conf.*, Bedford, MA, 1998.

[5] A. M. Monk, M. Davis, L. B. Milstein, and C. W. Helstrom, "A noise-whitening approach to multiple access noise rejection—Part I: Theory and background," *IEEE J. Select. Areas Commun.*, vol. 12, pp. 817–827, June 1994.

[6] ——, "A noise-whitening approach to multiple-access noise rejection in a CDMA system," in *Proc. IEEE National Telesystems Conf.*, 1994, pp. 207–210.

[7] M. Davis, A. M. Monk, and L. B. Milstein, "A noise whitening approach to multiple-access noise rejection—Part II: Implementation issues," *IEEE J. Select. Areas Commun.*, vol. 14, pp. 1488–1499, Oct. 1996.

[8] T. F. Wong, T. M. Lok, and J. S. Lehnert, "Asynchronous multiple-access interference suppression and chip waveform selection with aperiodic random sequences," *IEEE Trans. Commun.*, vol. 47, pp. 103–114, Jan. 1999.

[9] T. F. Wong, T. M. Lok, J. S. Lehnert, and M. D. Zoltowski, "A linear receiver for direct-sequence spread-spectrum multiple-access systems with antenna arrays and blind adaptation," *IEEE Trans. Info. Theory*, vol. 44, pp. 659–676, Mar. 1998.

[10] Y. C. Yoon and H. Leib, "Matched filters for locked and unlocked interferers in DS-CDMA," in *Proc. IEEE Pacific Rim Conf. Commun.*, 1995, pp. 449–452.

[11] ——, "Matched filters with interference suppression capabilities for DS-CDMA," *IEEE J. Select. Areas Commun.*, vol. 14, pp. 1510–1521, Oct. 1996.

[12] A. Klein, "Multi-user detection of CDMA signals—Algorithms and their application to cellular mobile radio," Ph.D. thesis, University Kaiserslautern, Germany, 1996.
[13] ——, "Data detection algorithms specially designed for downlink of CDMA mobile radio systems," in *Proc. IEEE Veh. Technol. Conf.*, 1997, pp. 203–207.
[14] G. E. Bottomley, "Optimizing the RAKE receiver for the CDMA downlink," in *Proc. IEEE Veh. Technol. Conf.*, Secaucus, NJ, 1993, pp. 742–745.
[15] S. M. Kay, *Fundamentals of Statistical Signal Processing. Volume 2: Detection Theory*. Upper Saddle River, NJ: Prentice-Hall, 1998.
[16] M. Pursley, D. Sarwate, and W. Stark, "Error probability for direct-sequence spread-spectrum multiple-access communications—Part I: Upper and lower bounds," *IEEE Trans. Commun.*, vol. COM-30, pp. 975–984, May 1982.
[17] 3rd Generation Partnership Project, *TSG RAN WG4 UE Radio Transmission and Reception (FDD)*, June 1999. version 2.0.0.

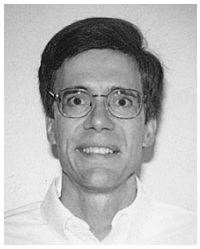

Gregory E. Bottomley (S'81–M'85–SM'99) received the B.S. and the M.S. degrees from Virginia Polytechnic Institute and State University, Blacksburg, in 1983 and 1985, respectively, and the Ph.D. degree from North Carolina State University, Raleigh, in 1989, all in electrical engineering.

From 1985 to 1987, he was with AT&T Bell Laboratories, Whippany, NJ, working in the area of sonar signal processing. In 1990, he was a Visiting Lecturer at North Carolina State University, Raleigh. Since 1991, he has been with Ericsson Inc., Research Triangle Park, NC, where he is currently a Senior Consulting Engineer in the Advanced Development and Research Department. His research interests are in baseband signal processing for mobile communications, including equalization, RAKE reception, and interference cancellation.

Dr. Bottomley is a member of Sigma Xi and, since 1997, an Associate Editor for the IEEE TRANSACTIONS ON VEHICULAR TECHNOLOGY.

Tony Ottosson (S'93–M'98) was born in Uddevalla, Sweden, in 1969. He received the M.Sc. in electrical engineering from Chalmers University of Technology, Göteborg, Sweden, in 1993, and the Lic.Eng. and Ph.D. degrees from the Department of Information Theory, Chalmers University of Technology, in 1995 and 1997, respectively.

Currently he is an Associate Professor in the Communication Systems Group, Department of Signals and Systems, Chalmers University of Technology. During 1999, he was also working as a Research Consultant at Ericsson Inc., Research Triangle Park, NC USA. From October 1995 to December 1998, he participated in the European FRAMES (Future Radio wideband Multiple Access System) project both as a co-worker and during 1998 as Activity Leader of the area of coding and modulation.

His research interests are in communication systems and information theory and are mainly targeted to CDMA systems. Specific topics are modulation, coding, multirate schemes, multiuser detection, combined source-channel coding, joint decoding techniques, and synchronization.

Yi-Pin Eric Wang (S'91–M'96) received the B.S. degree in electrical engineering from National Taiwan University in 1988, and the M.S. and Ph.D. degrees, both in electrical engineering, from the University of Michigan, Ann Arbor, in 1991 and 1995, respectively.

He has been a member of the Advanced Development and Research Group of Ericsson Inc. in Research Triangle Park, NC USA, since 1995. His work focuses on wireless communications, including mobile satellite communication systems and terrestrial cellular systems. His research interests include coding, modulation, synchronization, and interference cancellation in CDMA systems.